






---

## FABRICATION OF OLEOGELS VIA OIL ABSORPTION IN AEROGEL TEMPLATES OF CELLULOSE AND STARCH

Laiane Carvalho<sup>(a)</sup>, Larissa Andreani Carvalho<sup>(b)</sup>, Sandra Maria da Luz<sup>(c)</sup>, Simone Monteiro e Silva<sup>(d)</sup>, Leonardo Fonseca Valadares<sup>(e)\*</sup>

- (a)  0009-0003-6110-2721 (University of Goiás – Brazil)  
(b)  0000-0002-6567-5725 (Embrapa Agroenergia – Brazil)  
(c)  0000-0002-2223-0021 (University of Brasília – Brazil)  
(d)  0000-0002-2774-1656 (University of Brasília – Brazil)  
(e)\*  0000-0002-4190-8598 (Embrapa Agroenergia - Brazil)

CODE: BCCM7-150

**Keywords:** Bioaerogels, Microfibrillated Cellulose, Cotton, Composite, Freeze Drying

**Abstract:** The oleogelation technique is one innovative method applied for oil structuring and producing the so-called oleogels, which have the potential for various applications, such as reduce trans and saturated fats in foods and drug delivery. Several methods and/or combinations of them can be used to promote oleogelation and are usually divided into direct dispersion and indirect methods, such as emulsion, solvent exchange, and porous solid materials, such as foams and aerogels. Aerogels are solid materials with high specific surface area, high porosity, and very low density, which is suitable for oil sorption. In this work, pure and composites aerogels of potato starch and microfibrillated cotton cellulose were prepared via freeze-drying and tested as templates for oleogel. The increase in starch concentration increases the density and reduces the porosity of the aerogel as consequence of the higher solids content in the aqueous dispersions. The composites showed the morphology of conglomerates and planar aggregates, but superior mechanical properties compared to pure biopolymers, with improvement in elastic modulus and plasticity, as well as greater thermal stability. The higher oil absorption capacity was observed on pure cellulose aerogel (179.42 g/g). Although the addition of starch reduced the absorption capacity of the composites, they have excellent absorption capacities, ranging from 18.95 to 55.59 g/g and an oil holding capacity of up to 81.54%. These results show that cellulose and starch aerogels, hydrophilic polysaccharides, can be used to structure oil and produce oleogel indirectly by the oil sorption mechanism, having potential for oil absorption and delivery.

---

### 1. INTRODUCTION

The oleogelation is particularly a technique with potential for structuring fats, transforming edible liquid oil into a solid gel using structuring agents, forming the so-called oleogels. Oleogels are defined as semi-solid systems resulting from the trapping of liquid oil in a three-dimensional lattice without modifying the chemical characteristics of the oil [1]. Typically, oleogels are induced by structuring agents or oleogelators that can be low molecular weight, such as wax, lecithin, esters, and ceramides, and high molecular weight, such as proteins and polysaccharides [2]. Oleogels combine the nutritional profile of liquid oils and the functionality of solidified fats without using high levels of saturated fatty acids. In addition to food nutrition, these materials have been studied in various processes such as delivery of active compounds and oil treatment [3,4].

Several methodologies can be employed for the preparation of oleogels, which include the use of foams or aerogels as templates to trap the oil. Aerogels are solid materials produced by supercritical drying of CO<sub>2</sub> or by freeze-drying, with characteristics such as high porosity and low density, which is suitable for oil

sorption. Among the various sources, polysaccharide aerogels (e.g., cellulose, chitosan, alginate, starch, agar etc.) have received the most attention. In this sense, cellulose and starch stand out for being the most abundant biopolymers and are mostly GRAS (Generally Recognized As Safe). However, the aerogels of pure cellulose or pure starch have some disadvantages: cellulose, despite having bending properties, have a soft structure and deforms easily, while pure starch aerogel has inferior mechanical properties and high hydrophilicity [5]. Therefore, although the study on cellulose and starch composite aerogels is incipient, some studies suggest that the production of aerogels from the mixture of these two biopolymers can modulate the properties of the final material.

Thus, the objective of this work was to study the properties of aerogels based on starch and microfibrillated cellulose (MFC) and oleogels produced by them indirectly from oil absorption.

## 2. METHODOLOGY

Commercial hydrophilic cotton was obtained from Farol (Minas Gerais, Brazil). Potato starch (product reference: S2004) was purchased from Sigma Aldrich (Bangalore, India). The soybean oil was purchased in a local market. Distilled water was used to prepare the hydrocolloids. The other reagents used in the experiments were of analytical grade.

Initially, the precursor materials of the aerogel were prepared: microfibrillated cellulose and gelatinized starch. An aqueous dispersion of cellulose of approximately 0.25 % (w/w) was produced by shearing cotton in a blender (Britannia, BLQ1280, 1150W) with a filter attached. After all the cotton had been dispersed, the shearing of the cellulose proceeded in an Ultra-turrax homogenizer (IKA, T25 D S32) in 10 cycles of 5 min at the speed of 18,000 rpm. Gelatinized starch was produced by mixing soluble potato starch in distilled water at the proportion of 4% (w/w). Then, the mixture was kept at 70 °C with constant stirring in a water bath for 30 minutes.

The aerogels were produced with the following cellulose/starch compositions: 100/0, 80/20, 50/50, 20/80 and 0/100. To form the composites, the two polymers were mixed in those proportions with the Ultra-turrax at the speed of 15,000 rpm for 1 minute, to homogenize the mixture. Then, the hydrogels were added in Petri dishes and Falcon tubes for molding into the shape of monoliths, and frozen in a -18 °C freezer for 24 hours and for a further four hours in the freezer at -80 °C. Finally, the material was dried in a freeze dryer (LIOTOP, K120) for 96 hours at -93 °C and 300 µHg. The oleogels were obtained by immersing the aerogel monoliths in soybean oil for 5 minutes, which ensured their saturation.

The aerogels were characterized for their apparent density ( $\rho_a$ ), porosity (P) and volumetric shrinkage (VS), according to the following equations:

$$\rho_a = \frac{m}{V} \quad (1)$$

$$VS = \frac{V_d - V}{V_d} \quad (2)$$

$$P = 1 - \frac{\rho_a}{\rho_b} \Rightarrow P = 1 - \rho_a \times \left( \frac{w_{cellulose}}{\rho_{cellulose}} - \frac{w_{starch}}{\rho_{starch}} \right) \quad (3)$$

where m is the mass and V is the volume of the aerogel,  $V_d$  is the volume of the dispersion,  $w_{cellulose}$  and  $w_{starch}$  is the mass fraction of the cellulose and starch in the aerogel, respectively,  $\rho_{cellulose}$  is the density of the cellulose and  $\rho_{starch}$  is the density of the starch. According to the literature, the cellulose density of cotton fiber is 1.50 g.cm<sup>-1</sup> and the density of potato starch is equal to 1.45 g.cm<sup>-1</sup> [6].

The aerogels were characterized as for the morphology (JEOL, JSM 7001F), crystallinity (Bruker, D8 FOCUS), chemical interaction (Shimadzu, Affinity-1), mechanical properties (Arotec, WDW-20E) and thermal properties (TA Instruments, SDT Q600).

### 3. RESULTS AND DISCUSSION

#### 3.1. Physical properties of the aerogels

The values of bulk density, porosity and volumetric shrinkage of pure and composite aerogels can be seen in Table 1.

**Table 1.** The physical characteristics of the aerogels.

Sample	Solid content (%)	$\rho_0$ (g.cm <sup>-3</sup> )	P (%)	VS (%)
S0C100	0.25	0.003 ± 0.000 <sup>a</sup>	99.8 ± 0.2 <sup>a</sup>	30.5 ± 0.5 <sup>a</sup>
S20C80	1.00	0.013 ± 0.000 <sup>b</sup>	99.1 ± 0.3 <sup>b</sup>	31.2 ± 1.5 <sup>a</sup>
S50C50	2.13	0.030 ± 0.001 <sup>c</sup>	98,0 ± 0.5 <sup>c</sup>	33.1 ± 1.5 <sup>a</sup>
S80C20	3.25	0.047 ± 0.000 <sup>d</sup>	96.8 ± 0.2 <sup>d</sup>	33,7 ± 0.4 <sup>a</sup>
S100C0	4.00	0.056 ± 0.002 <sup>e</sup>	96.2 ± 0.2 <sup>e</sup>	33.0 ± 1.9 <sup>a</sup>

$\rho_0$  = bulk density, P = porosity and VS = volumetric shrinkage.

Results are expressed as mean values ± standard deviation of triplicate. Different superscript letters within the same column represent significant difference ( $p < 0.05$ ).

The apparent density of the aerogels was in the range of 0.003 and 0.056 g.cm<sup>-3</sup>, and the porosity between 96.2 and 99.8%. As expected, a lower solids content in the aqueous dispersion used to produce the aerogels resulted in a less dense and more porous structure. This inverse ratio between solids content and porosity can be explained by the increase in bonds with increased solids content between starch and cellulose in the same volume [7]. In the production of aerogels, it is also common to observe a decrease in volume after freeze-drying. This is due to several factors, such as the removal of the solvent (water), the composition and the degree of gelling of the precursor material [8]. Thus, the volumetric shrinkage (VS) can be used as a macroscopic indicative of the polymeric matrix stability during aerogel production [9]. The volumetric shrinkage of all aerogels was relatively close, ranging from 30.5% to 33,0%. In addition, it is possible to verify in the aerogels with higher levels of cellulose a lower volumetric reduction, which can be explained by the greater distance between the fibers in the aqueous matrix, leading to the formation of more open interconnected networks. A representative set of SEM images of the aerogels is shown in Fig. 1.

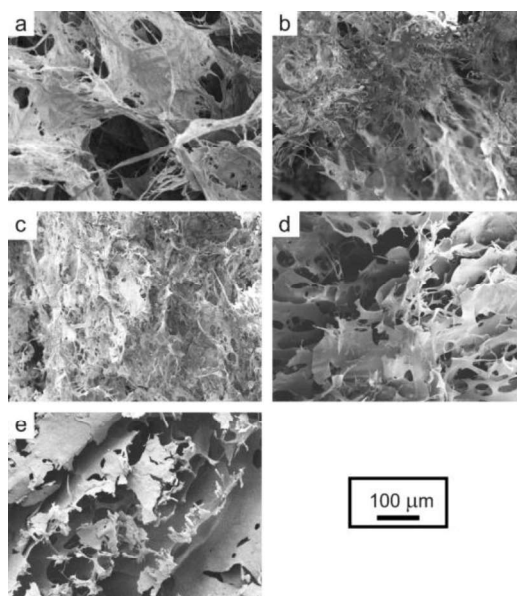


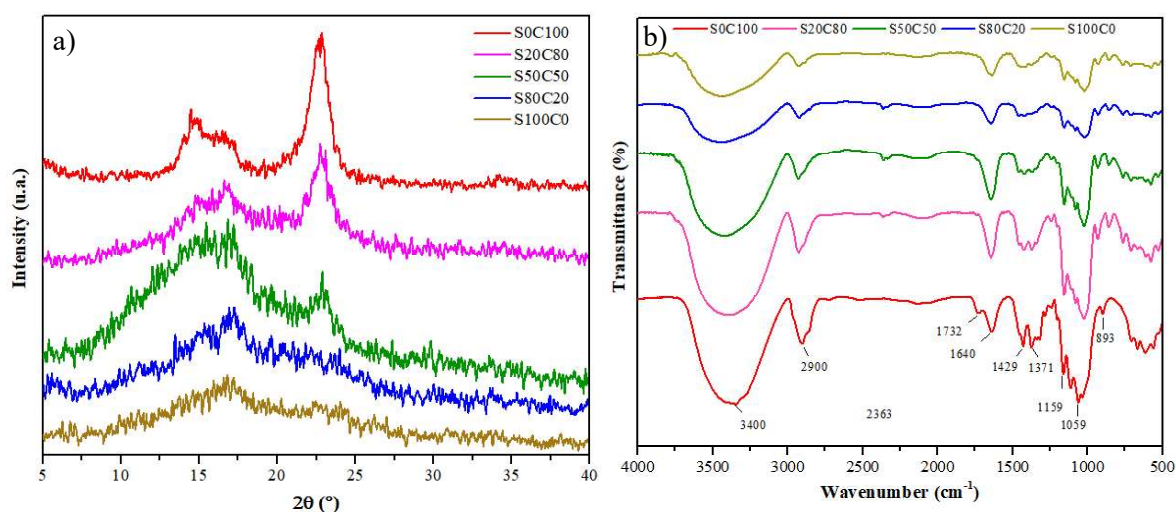
**Figure 1.** Scanning electron microscopy images of the aerogels a) S0C100, b) S20C80, c) S50C50, d) S80C20 and e) S100C0.

It is observed from pure cellulose aerogel variations in the diameters of the fibrils, which is due to both the raw material (mechanically produced MFC) and the production process (freeze-drying). Some cracks are evident due to the cellulose preparation process. Moreover, pure cellulose aerogel has the shape of three-

dimensional networks formed by web-like structures, which is justified by the action of capillary forces and hydrogen bonds between hydroxyl groups during freezing and freeze-drying [10]. In aerogels with low and intermediate starch concentrations (Figs 1b and c), conglutinated structures are observed with fibrils embedded within the starch matrix and this possibly allowed the cellulose fibers to be coated and protected from capillary forces during freezing and drying. On the other hand, with a higher concentration of starch (Figs 1d and e), there are more compact and dense structures, in the shape of leaves. The leaf-like structures are usually attributed to the slow growth of water crystals that compress the gel lattice into planar aggregates [11]. The microstructure of aerogels is related to the viscosity of the gel, so that less viscous gels have less resistance to the formation of ice crystals, allowing the formation of lamellar ice layers [12].

Fig. 2 shows the X-ray diffraction (XRD) patterns of the aerogels and some differences with respect to crystallinity are observed. As expected, the pure cellulose material presents diffraction peaks referring to the presence of a crystalline structure at  $2\theta \approx 22.9^\circ$  due to the crystalline plane (200), and the overlapping peaks  $11\bar{0}$  and  $110$  ( $14.8^\circ$  and  $16.7^\circ$ , respectively), characteristic of cellulose polymorph I [13]. It is verified that these peaks decrease with the addition of starch, not being observed in the S100C0 sample, which indicates that the starch in the aerogels is amorphous, due to the rupture of the granules during the gelatinization process.

Despite small differences between them, the FTIR spectra of the aerogels show the general characteristic spectrum of cellulose and starch (Fig 2.). Characteristic bands were detected at  $3400\text{ cm}^{-1}$  and  $2900\text{ cm}^{-1}$ , and were attributed to O–H and C–H stretching vibrations, respectively [14]. A peak at  $1732\text{ cm}^{-1}$  was observed in the pure cellulose spectrum, which is attributed to the vibration of C=O [15]. The peak at  $1640\text{ cm}^{-1}$  was related to the flexural vibrations of the adsorbed water [16]. The band at  $1429\text{ cm}^{-1}$  is attributed to  $\text{CH}_2$  deformation vibration which is a type of the "crystallinity band" of cellulose [14]. In addition, the sharp peak at  $1371\text{ cm}^{-1}$  reflects asymmetric C–H deformations. The band at  $1159\text{ cm}^{-1}$  corresponds to the C–O–C stretch of the  $\beta$ -1,4-glycosidic bond. A sharp and strong band at  $1059\text{ cm}^{-1}$  has been assigned to C–O stretch in cellulose, hemicellulose, and lignin or C–O–C stretch in cellulose and hemicellulose [15]. C–H vibration of cellulose which corresponds to the  $\beta$ -glycosidic linkage occurs at  $895\text{--}901\text{ cm}^{-1}$  [16].



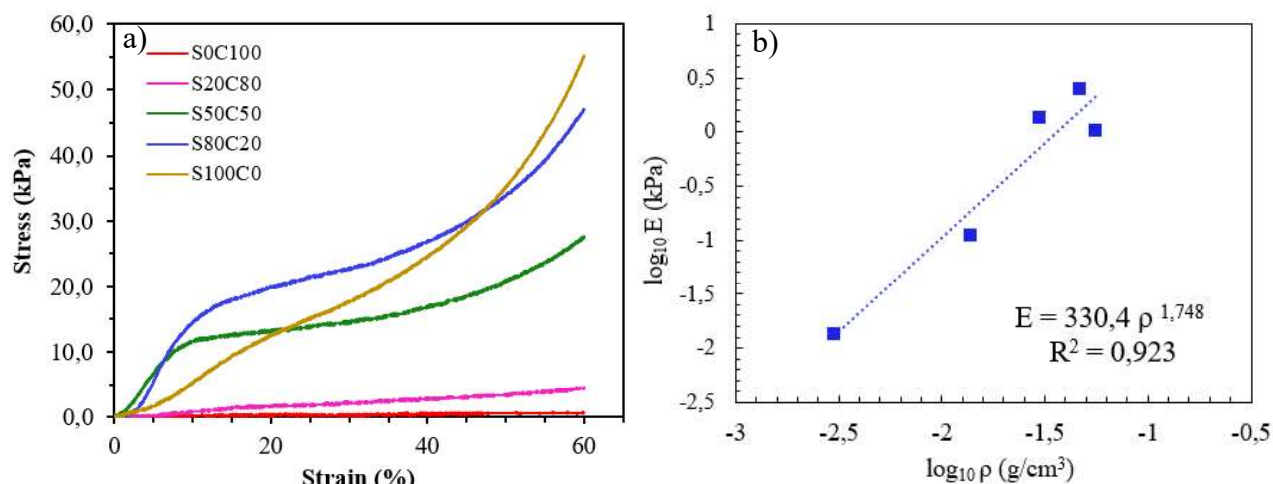
**Figure 2.** a) X-ray diffraction (XRD) and b) FTIR spectra of the pure and composite aerogels.

Fig. 3a shows the stress-strain curves of the aerogels with characteristic behavior of porous material, with the presence of the three regions normally found for biopolymer-based aerogels: elastic region, plastic region and densification region [17]. The increase in the solids content and, therefore, in the density of the aerogels correlated with the modulus of elasticity and tensile strength. Nonetheless, the pure starch aerogel (S100C0) exhibited low mechanical properties. The addition of microfibrillated cellulose (MFC) produced better flexural properties, acting as a reinforcement to the starch aerogel. This finding was probably due to good dispersion and the micron size of cellulose that allowed an effective contact area with the starch matrix [14].

Specifically, the S80C20 aerogel curve presents the highest inclination in all regions (elastic, plastic and densification), presenting the highest elastic modulus and the highest yield stress compared to the other pure and composite aerogels, indicating the more elastic characteristic. On the other hand, the aerogel containing the same proportions of cellulose and starch (S50C50) was less elastic and more plastic, with a greater extension of the plateau region. These two aerogels suggest that, while the addition of starch gives

elasticity to the aerogel, cellulose adds plasticity and in small amounts is already sufficient to act as a reinforcement for the aerogel predominantly composed of starch.

The compressive modulus ( $E$ ) generally depends on density according to the simple scaling law  $E \sim \rho^\alpha$  for aerogel materials (Fig. 3b), where the scaling exponent  $\alpha$  typically ranges from 1 to 4, depending on the network material and structure [18]. The exponent  $\alpha$  reflects the microstructures typically observed for each system. As can be seen in Fig. 3,  $\alpha = 1.748$  for the aerogels produced in this work. This value is consistent with that reported by other work for cellulose nanofiber aerogels, in which  $\alpha = 1.8$ . The exponent around 2 has also been reported for other polysaccharide-based aerogels (1.6 for chitosan and 1.9 for xanthan) [19]. These values are attributed to the predominantly foam-like structures, i.e., regular open cell structure, observed in most cellulose aerogels [18].



**Figure 3.** a) Stress vs strain curves and b) Young's Modulus ( $E$ ) as a function of bulk density ( $\rho$ ) of the aerogels.

The thermogravimetric curves (TGA and DTG) and DSC of the samples of pure microfibrillated cellulose, pure starch and cellulose/starch composites are shown in Fig. 4. Starch aerogels and their composites exhibited higher water loss at the initial stages of the process compared to the pure cellulose aerogel. This outcome aligns with expectations, considering the inherently hydrophilic nature of starch. The onset temperature of all aerogels was lower than the of pure cellulose aerogel, indicating that the addition of starch contributes to reduce thermal stability. Nevertheless, during the heating of the samples from 20 to 600 °C under a nitrogen atmosphere, S0C100 and S100C0 exhibited residual weights of 11.09% and 19.68%, respectively. This difference can be attributed to the increased condensation in the starch aerogel, enhancing its resistance to degradation. In contrast, the cellulose aerogel, being more porous and featuring an expanded contact surface due to the microfibrillation process, was more susceptible to thermal degradation [20]. Particularly, the residue of S80C20 surpassed all other aerogels, signifying that this blend of cellulose and starch offers enhanced thermal stability. This observation can be attributed to the improved structural and spatial arrangement facilitated by the interaction between fibers and starch in this specific composition.

In the DTG curves, four mass loss stages were identified, with peaks of varying intensities among the aerogels. The first stage occurs at low temperatures (less than 100 °C) and is attributed to the evaporation of water adsorbed on the material. The second stage was identified only in the samples with the highest starch contents (S80C20 and S100C0) in the range of 230-250 °C, which indicates starch degradation. The third stage of mass loss can be clearly observed in the DTG curves in the range of 250-310 °C, which is due to starch degradation and burning, and in the range of 250-390 °C due to cellulose degradation. The curves of the aerogels show a single endothermic peak, indicating a good interaction between the cellulose fibers and the starch matrix. Composite aerogels showed higher  $T_m$  value (65.39-70.68 °C) than pure aerogels (51.59-54.68 °C), suggesting a significant improvement in thermal stability. This can be attributed to the interactions between starch and cellulose, resulting in a decrease in the mobility of macromolecules. In addition, the enthalpy of degradation (14.64-75.53 J/g) increases with the addition of starch, with the opposite effect for cellulose, probably due to the reduction of crystallinity, increasing thermal resistance and, consequently, requiring more energy for degradation.

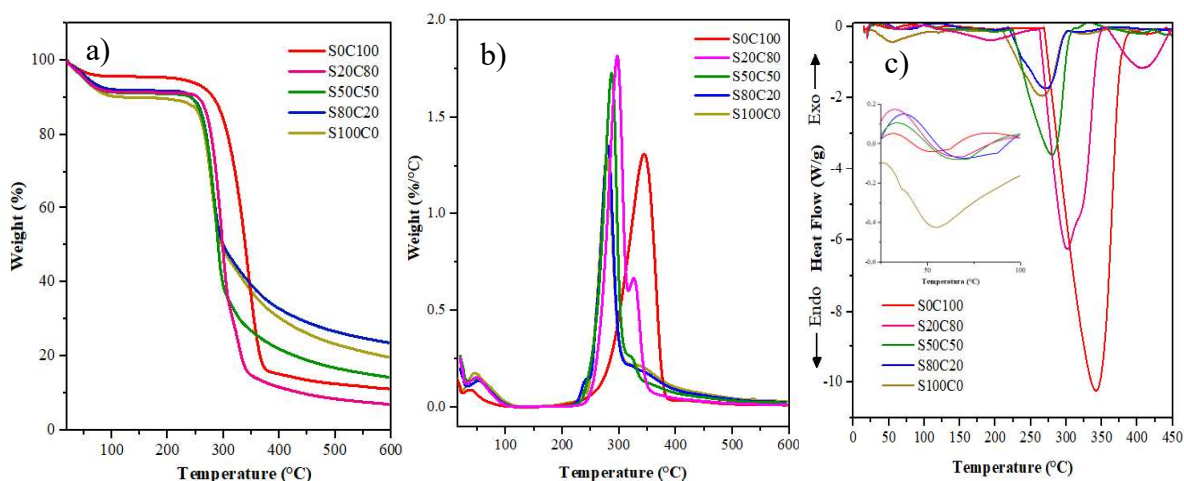


Figure 4. (a) TGA, b) DTG and c) DSC curves of the aerogels.

### 3.2. Oleogel characterizations

Oleogels are mainly characterized by the oil absorption and oil holding capacity, hardness, rheological and thermal properties. As shown in Table 2, all aerogels showed a good absorption capacity. The addition of starch to cellulose reduced the oil absorption capacity, being higher for pure cellulose aerogel (S0C100) with 179.42 g/g and lower for pure starch aerogel (S100C0) with 14.76 g/g. This significant difference between the aerogels was possibly because the oil-trapping ability of the aerogels was affected not only by the properties of the biopolymer, since cellulose is amphiphilic, but also by the organization of the polymer network and its internal architecture [1].

The Fig 5. presents the digital photographs of the aerogels and oleogels. In aerogels with higher starch concentrations, density increases, resulting in fewer pores and, consequently, reduced ability to trap oil. However, the addition of starch significantly influenced the structuring of the oil, with aerogels having the highest starch content exhibiting the highest oil retention. The oil holding capacity of the S0C100 oleogel was very poor because the network strength of the S0C100 aerogel was too weak due to the lowest hardness, and the network structure of the S0C100 oleogel would be most likely to be destroyed with the external force, resulting in a large amount of the oil leakage in the oleogel (Fig. 5).

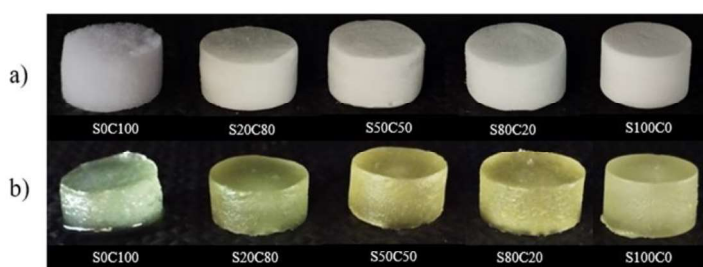


Figure 5. Digital photographs of the aerogels (a) before and (b) after absorbing oil.

The Table 2 presents the oil adsorption and oil holding capacity and the hardness of the oleogels. The combination of starch and cellulose fibers appears to have an optimal point where the upper structural arrangement retains more oil, exemplified by S50C50 (81.54%). The higher oil retention observed may be related to the greater plasticity of the aerogel, as observed in the stress vs strain curve of both the aerogel and the oleogel (Fig. 3a and Fig 6), since the plasticity allows the oleogel to adapt to different conditions, such as temperature and pressure. Thus, it can be inferred that this combination of biopolymers, in particular, results in a more synergistic oleogelator system. Predominantly, the hardness of oleogels is assessed by penetration/compression measurements. The values obtained from the compression of the oleogels indicate that the hardness is directly related to the increase in the solids content, as expected. This may explain the higher oil-holding capacity for aerogels with higher starch concentrations, as the structure becomes more enclosed and able to trap more oil.

**Table 2.** Oil adsorption capacity and oil holding capacity of the aerogels and hardness of oleogel.

Sample	Oil absorption capacity (g/g)	Oil holding capacity (%)	Hardness of oleogel (N)
S0C100	179.42 ± 2.59 <sup>a</sup>	56.55 ± 4.59 <sup>d</sup>	0.22 ± 0.08 <sup>d</sup>
S20C80	55.59 ± 1.76 <sup>b</sup>	66.78 ± 5.36 <sup>b</sup>	0.96 ± 0.34 <sup>c</sup>
S50C50	29.74 ± 1.30 <sup>c</sup>	81.54 ± 1.29 <sup>a</sup>	5.00 ± 0.46 <sup>b</sup>
S80C20	18.95 ± 0.66 <sup>d</sup>	74.94 ± 2.36 <sup>ab</sup>	13.28 ± 4.63 <sup>a</sup>
S100C0	14.76 ± 0.62 <sup>c</sup>	79.55 ± 2.05 <sup>a</sup>	15.28 ± 2.98 <sup>a</sup>

Results are expressed as mean values ± standard deviation of triplicate. Different superscript letters within the same column represent significant difference ( $p < 0.05$ ).

The stress vs strain curves obtained in the oleogel compression test are shown in Fig. 6. It is observed that the hardness or compressive strength of oleogels is proportional to the solids content (i.e., the addition of starch content). In addition, with the increment of starch, the oleogel presents an increase in the elastic region, with an inverse relationship for cellulose, which, in this turn, confers greater plasticity to the oleogel. This result is consistent with the work of Gravelle (2017), who showed an improvement in the plasticity of the oleogel with the addition of ethyl cellulose (Fig. 6).

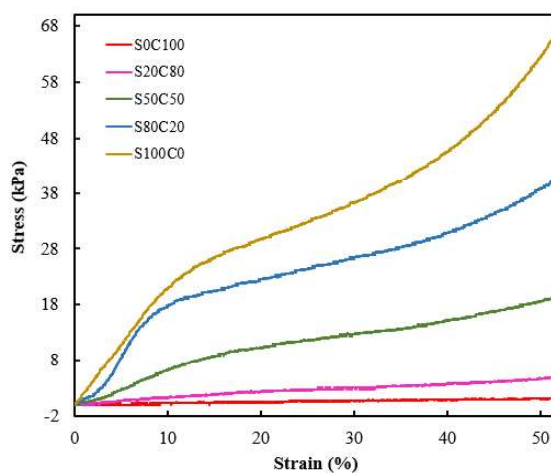


**Figure 6.** Stress vs strain curves of the oleogels obtained from the compression tests.

#### 4. CONCLUSIONS

In this work, aerogels from pure cellulose and starch and its composites were prepared from microfibrillated cellulose from cotton and potato starch and were transformed into oleogels via oil sorption. Compared to pure biopolymer aerogels, composite aerogels showed good mechanical properties and thermal stability. These aerogels are able to absorb considerable amounts of oil with high oil-holding capacity in the form of oleogels. In addition, the starch concentration significantly influenced the mechanical strength and the holding capacity of the oil, while the cellulose added mechanical flexural properties, such as plasticity, acting as a reinforcement to the aerogel. In summary, this work presented a simple approach to the production of oleogels, without the use of chemical reactions and temperature, only by immersing the aerogels in oil. These results suggest that cellulose and starch-based aerogels can be used to absorb lipophilic molecules, suggesting promising applications, including the control oil spills. Meanwhile, oleogels can be employed in various areas such as food and pharmaceuticals, as all material used are GRAS.

##### 4.1. Declaration of Competing Interest

The authors declare no conflict of interest.

##### 4.2. Fundings

This work was supported by the Brazilian funding agency Foundation for Research Support of the State of Goiás (FAPEG), project number SBO2022021000023. This is a contribution to Biofibras Project (SEG 20.19.053.00.00)

## 5. REFERENCES

- [1] Manzocco L, Valoppi F, Calligaris S, Andreatta F, Spilimbergo S, Nicoli MC. Exploitation of  $\kappa$ -carrageenan aerogels as template for edible oleogel preparation. *Food Hydrocoll* 2017;71:68–75. <https://doi.org/10.1016/j.foodhyd.2017.04.021>.
- [2] Li J, Zhang C, Li Y, Zhang H. Fabrication of aerogel-templated oleogels from alginate-gelatin conjugates for in vitro digestion. *Carbohydr Polym* 2022;291. <https://doi.org/10.1016/j.carbpol.2022.119603>.
- [3] Abdullah, Zou YC, Farooq S, Walayat N, Zhang H, Faieta M, et al. Bio-aerogels: Fabrication, properties and food applications. *Crit Rev Food Sci Nutr* 2022;0:1–23. <https://doi.org/10.1080/10408398.2022.2037504>.
- [4] Yang WJ, Yuen ACY, Li A, Lin B, Chen TBY, Yang W, et al. Recent progress in bio-based aerogel absorbents for oil/water separation. *Cellulose* 2019;26:6449–76. <https://doi.org/10.1007/s10570-019-02559-x>.
- [5] Ago M, Ferrer A, Rojas OJ. Starch-Based Biofoams Reinforced with Lignocellulose Nanofibrils from Residual Palm Empty Fruit Bunches: Water Sorption and Mechanical Strength. *ACS Sustain Chem Eng* 2016;4:5546–52. <https://doi.org/10.1021/acssuschemeng.6b01279>.
- [6] Paulauskiene T, Teresiute A, Uebe J, Tadzijevas A. Sustainable Cross-Linkers for the Synthesis of Cellulose-Based Aerogels: Research and Application. *J Mar Sci Eng* 2022;10. <https://doi.org/10.3390/jmse10040491>.
- [7] Yildirim N, Shaler SM, Gardner DJ, Rice R, Bousfield DW. Cellulose nanofibril (CNF) reinforced starch insulating foams. *Cellulose* 2014;21:4337–47. <https://doi.org/10.1007/s10570-014-0450-9>.
- [8] Payanda Konuk O, Alshihle AAAM, Yousefzadeh H, Ulker Z, Bozbag SE, García-González CA, et al. The effect of synthesis conditions and process parameters on aerogel properties. *Front Chem* 2023;11:1–26. <https://doi.org/10.3389/fchem.2023.1294520>.
- [9] Mehling T, Smirnova I, Guenther U, Neubert RHH. Polysaccharide-based aerogels as drug carriers. *J Non Cryst Solids* 2009;355:2472–9. <https://doi.org/10.1016/j.jnoncrysol.2009.08.038>.
- [10] Chen W, Yu H, Li Q, Liu Y, Li J. Ultralight and highly flexible aerogels with long cellulose i nanofibers. *Soft Matter* 2011;7:10360–8. <https://doi.org/10.1039/c1sm06179h>.
- [11] Baudron V, Gurikov P, Smirnova I, Whitehouse S. Porous starch materials via supercritical-and freeze-drying. *Gels* 2019;5:9–13. <https://doi.org/10.3390/gels5010012>.
- [12] Chen W, Abe K, Uetani K, Yu H, Liu Y, Yano H. Individual cotton cellulose nanofibers: Pretreatment and fibrillation technique. *Cellulose* 2014;21:1517–28. <https://doi.org/10.1007/s10570-014-0172-z>.
- [13] Nindiyasari F, Griesshaber E, Zimmermann T, Manian AP, Randow C, Zehbe R, et al. Characterization and mechanical properties investigation of the cellulose/gypsum composite. *J Compos Mater* 2015;50:657–72. <https://doi.org/10.1177/0021998315580826>.
- [14] Nordin N, Othman SH, Kadir Basha R, Abdul Rashid S. Mechanical and thermal properties of starch films reinforced with microcellulose fibres. *Food Res* 2018;2:555–63. [https://doi.org/10.26656/fr.2017.2\(6\).110](https://doi.org/10.26656/fr.2017.2(6).110).
- [15] Li D, Zhu FZ, Li JY, Na P, Wang N. Preparation and characterization of cellulose fibers from corn straw as natural oil sorbents. *Ind Eng Chem Res* 2013;52:516–24. <https://doi.org/10.1021/ie302288k>.
- [16] Abidi N, Cabrales L, Haigler CH. Changes in the cell wall and cellulose content of developing cotton fibers investigated by FTIR spectroscopy. *Carbohydr Polym* 2014;100:9–16. <https://doi.org/10.1016/j.carbpol.2013.01.074>.
- [17] Wang Y, Wu K, Xiao M, Riffat SB, Su Y, Jiang F. Thermal conductivity, structure and mechanical properties of konjac glucomannan/starch based aerogel strengthened by wheat straw. *Carbohydr Polym* 2018;197:284–91. <https://doi.org/10.1016/j.carbpol.2018.06.009>.
- [18] Zhao S, Malfait WJ, Guerrero-Alburquerque N, Koebel MM, Nyström G. Biopolymer Aerogels and Foams: Chemistry, Properties, and Applications. *Angew Chemie - Int Ed* 2018;57:7580–608. <https://doi.org/10.1002/anie.201709014>.
- [19] Buchtová N, Pradille C, Bouvard JL, Budtova T. Mechanical properties of cellulose aerogels and cryogels. *Soft Matter* 2019;15:7901–8. <https://doi.org/10.1039/c9sm01028a>.
- [20] Teles VC, Roldi M, Luz SM, Santos WR, Andreani L, Valadares LF. Obtaining Plasticized Starch and Microfibrillated Cellulose from Oil Palm Empty Fruit Bunches: Preparation and Properties of the Pure Materials and Their Composites 2021:3746–59.